

Ground-penetrating radar applied to imaging sheet joints in granite bedrock

Granitic rocks commonly develop exfoliation surfaces (also called as sheet joints), which are generally surface-parallel fracture systems. These structures may form in response to: (i) exhumation processes in which erosion causes upliftment of buried rocks; (ii) physical weathering due to thermal expansion and contraction; (iii) groundwater-related chemical weathering, and (iv) tectonic deformation. Although these structures are interesting geological features giving insights into past geological processes^{1,2}, they have several other implications for engineering geological applications and groundwater exploration. The exfoliation joints can transport large volumes of groundwater laterally for long distances in many directions. Geological mapping of these structures is possible only on cliff sections, whereas in the near surface they cannot be detected. Geophysical studies can greatly help in locating them in the subsurface. In this communication, we demonstrate the application of ground-penetrating radar (GPR) in detecting subsurface exfoliation joints in granite exposure area near Durgam Cheruvu, a micro-earthquake zone in Hyderabad (Figure 1). The findings would be helpful for planning underground excavation (e.g. construction of tunnels), modelling groundwater flow systems, and designing foundation structures of large-scale building structures.

Hyderabad area forms the northeastern extension of the Eastern Dharwar Craton, which is largely composed of ~2.7–2.5 Ga-old granites and gneisses with minor narrow tracts of meta-volcanic-sedimentary schist belts^{3,4}. Morphostructurally, this area is composed of near-circular granite massifs, which are approximately bounded by the Krishna and Manjeera rivers in the north and south respectively. It largely exposes Archaean medium to coarse-grained granites, porphyritic granites with small inclusions of amphibolites and migmatitic gneisses at places. Structural lineaments are abundant in and around Hyderabad. These lineaments are geomorphic valleys, river drainage systems and long-linear topographic highs on ground, with major orientations of N–S, NE–SW and ESE–WNW⁵.

The study area is near Durgam Cheruvu that experienced micro-earthquake events in 1994, 1995 and 1998 (refs 6 and 7). Geological analysis of granite exposures to the west and east of Durgam Cheruvu and KBR Park area (Figure 1) has shown the presence of numerous deformational structures such as foliations, fractures and brittle to ductile shear zones. Trends of the fractures and shear zones are NNE–SSW to NE–SW and E–W to ESE–WNW (Figure 1c), which are broadly similar to the regional lineament orientations. Near Durgam Cheruvu (Figure 1a), the streams marking the drainage flow along these fractures and shear zones, depicting a rectangular drainage pattern. The Durgam Cheruvu Lake lies at the intersection of the NNE–SSW and WNW–ESE-oriented faults, and the shape of the Lake is structurally controlled. Sheet joints are observed on

granite quarry cliffs near the northwestern part of KBR Park, which is ~3 km east of Durgam Cheruvu Lake (Figures 1 and 2). The quarry exposes porphyritic and coarse-grained granites with substantial weathering near the surface. Several near-horizontal sheet joints are abundant on the quarry wall (Figure 2). Many individual sheet joints occur in the form of steps with their tips connected by curved linkage zones. Joint spacing varies from a few millimetres to >1 m. Brecciation is common in the areas that are intersected by densely populated joints. Sheet joints also occur one below the other, appearing in the form of layers.

Although the quarry exposures suggest abundant sheet joints in the area, in order to detect them in the subsurface of the quarry surface, we selected two profiles (Figure 1b), one parallel to the quarry wall (P2) and the other perpendicular to

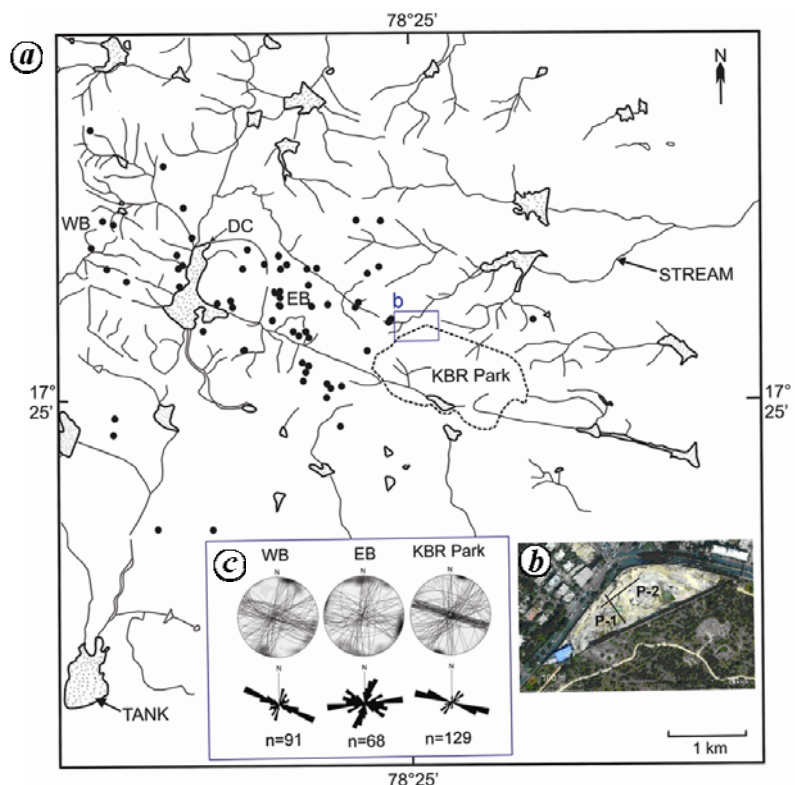


Figure 1. *a*, A drainage map of Durgam Cheruvu (DC) area showing location of micro-earthquakes. Geological observations were made on either sides of DC (WB and EB, western and eastern blocks respectively) and KBR Park area. *b*, Google satellite image showing location of the granite quarry, where ground-penetrating radar (GPR) data were obtained (P1; Profile 1; P2, Profile 2). *c*, Equal area plots and bi-directional rose diagrams showing fracture orientation data from WB, EB and KBR Park granite exposure areas.

it (P1). Good quality GPR data have been obtained along these profiles. The GPR equipment enabled rapid acquisition of subsurface image, producing a 2D time/depth section, at a rate of ~20 m/min. Jol⁸ provides a comprehensive review of GPR methods and earth science-related applications.

The length of the GPR profiles P1 and P2 is 57.5 and 72 m respectively. We used 400 MHz antenna (M/S GSSI, USA). The mode of acquisition was zero-offset with the transmitting and receiving antennae mounted on the same pack (monostatic mode). The acquired data consist of a number of traces with a spatial resolution of ~3 cm and two-way travel time record length of 60 ns. The GPR data were processed using PRISM2 software. In order to remove the background noise and improve the signal-to-noise ratio, a band-pass filter was used. Time-varying gains were applied (linear, spherical and exponential) to compensate the attenuation, spherical divergence and scattering of the radio signals. Frequency-wavenumber filtering was applied to remove the lateral reflections from the adjoining geological structures. As the survey site is nearly horizontal, the effect of topography on the geometry of the reflectors is not significant. To convert the time section into the depth section, a radar velocity of 0.13 m/ns was considered, assuming a dielectric constant value of 5.5 for the granite formations. The electromagnetic wave propagation in the subsurface material is related to the dielectric constant k , by the relation given by

$$v = C/\sqrt{k},$$

where C is the velocity of the electromagnetic wave in free space, which is 0.3 m/ns. For granite bedrock, the dielectric constant may vary from 5 to 8. For the present study, we considered a dielectric constant of 5.5 that provides a radar velocity of 0.13 m/ns. This velocity is consistent with the common midpoint (CMP) data that we obtained close to the survey area using 100 MHz bistatic antennas for offset varying from 1 to 14 m, with an increment of 0.5 m. The CMP data were processed using Radan and PRISM2 software by applying different processing modules. After processing the CMP data, velocity analysis was performed and the results show a mean velocity value of 0.13 m/ns. The final

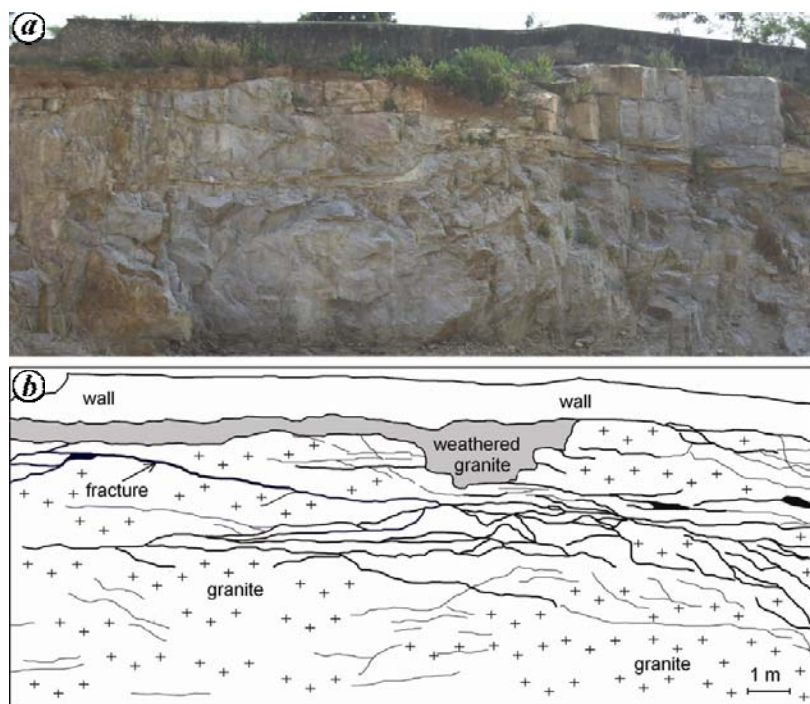


Figure 2. *a*, Photograph showing the southeastern cliff wall of granite quarry. *b*, Geological section showing the sheet joints; a thin weathering layer is also present on the top.

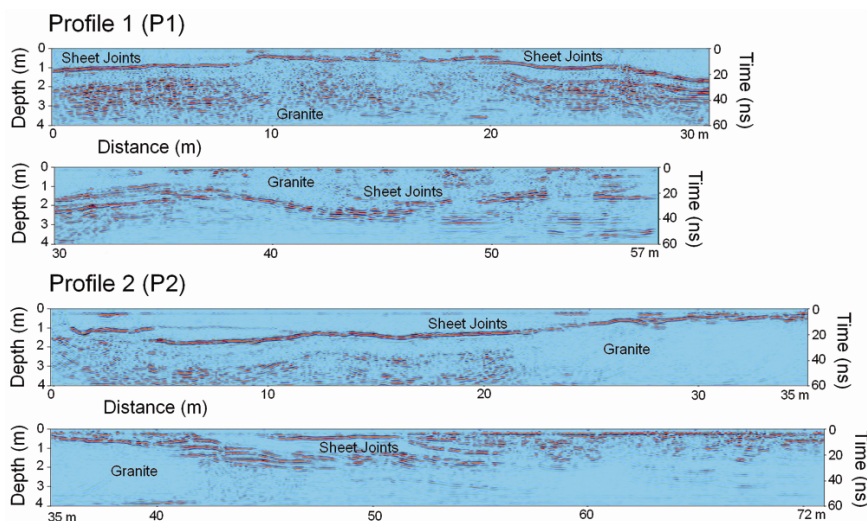


Figure 3. The 400 MHz GPR sections of P1 and P2. The sub-horizontal reflectors are interpreted to be sheet joints.

processed GPR sections P1 and P2 are shown in Figure 3.

Figure 3 shows many inclined to sub-horizontal reflectors throughout the section, but strong reflectors are abundant at 0.5–2 m depth range. The uppermost reflector is an undulating surface with disruption at few places. The upper reflector is underlain by a zone of multiple weak reflectors. We interpret that the granite bedrock is composed of layers of undu-

lating sheet joints, probably filled with groundwater. The lower zone of reflectors may be related to closely spaced sheet joints with substantial amount of brecciation and weathering. However, along P2, from 40 to 60 m distance range, the lower zone of reflectors is absent. We interpret that this may be due to the presence of fresh granite that is less affected by fracturing and weathering. The sheet joints also occur in the form of

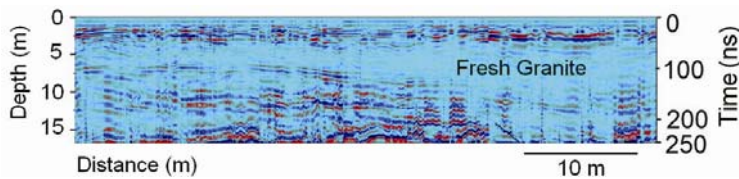


Figure 4. The 100 MHz GPR section of P1. The sub-horizontal reflectors are interpreted to be sheet joints. A slab of fresh granite occurs between two thick sheet-joint zones.

steps, for example, from 40 to 50 m distance range of P2. The GPR observations are similar to the observation from the quarry section, as shown in Figure 2. Therefore, our study provides strong evidence that GPR can efficiently be used for detecting sheet joints at the near surface.

In order to ascertain whether sheet joints can occur in the deeper levels beyond 4 m depth, we carried out another survey along P2 with the help of a 100 MHz GPR, considering the site suitability. The processed GPR section is shown in Figure 4. Unlike the 400 MHz sections (Figure 3), the 100 MHz section (Figure 4) provides a coarse resolution image of reflectors up to a depth >15 m. Two sets of reflectors are present; one set near the surface at a depth level of 2.5 m and the other beneath 7 m. The shallow reflectors can be related to the sheet joints seen in the 400 MHz sections (Figure 3). Additionally, the 100 MHz section shows deeper reflectors beyond 7 m up to a depth of ~16 m; these can also be ascribed to the deeper sheet joints. It is unknown whether sheet joints can be present beyond 16 m. Probably, usage of a 50 MHz frequency GPR may provide further clues.

Figures 3 and 4 have clearly shown that the study area has two broad zones of sheet joints, one in the shallower level (2–4 m depth) and the other in the deeper level (7–16 m depth). Between these two

layers, there exists a wedge of fresh granite (Figure 4). Detection of these structures can be useful in many applications. For example, sheet joints can be a potential groundwater reservoir that can spatially extend to long distances. Also, the groundwater can flow laterally to the extent of joints, probably in many directions. Therefore, the sheet joints are a unique structural discontinuity that distribute groundwater for large areas. In geo-engineering applications, the sheet joints are hazardous as they may lower the stability of structures. For example, during tunnelling operations, the sheet joints can lead to roof collapse. In a city like Hyderabad, where construction of underground metro railway or sewerage lines is being planned, it is essential to map the sheet joints in the subsurface. In New Delhi, the depth of tunnels of underground metro railway lines is in the depth range of 12–20 m at several places⁹. If the similar depth range is considered in Hyderabad, then it is important to take into account the presence of sheet joints and their potential impact on the stability of tunnel structures.

1. Twidale, C. R., *Rock Mech.*, 1973, **5**, 163–187.
2. Vidal Roman, J. R. and Twidale, C. R., *Geomorphology*, 1999, **31**, 13–27.
3. Chadwick, B., Vasudev, V. N. and Hegde, G. V., *Precambrian Res.*, 2000, **99**, 91–111.

4. Kumar, P. S. and Reddy, G. K., *Earth Planet. Sci. Lett.*, 2004, **224**, 309–324.
5. Seshunarayana, T., Satish Kumar, K., Deenanadh, S., Rama Mohan Rao, Y. and Senthil Kumar, P., In *Indian Dykes* (eds Srivastava, R. K., Sivaji, Ch. and Chalapati Rao, N. V.), Narosa Publishing House, New Delhi, 2008, pp. 331–338.
6. Rao, C. V. R. K. and Raju, P. S., *J. Geol. Soc. India*, 1996, **48**, 467–469.
7. Raju, P. S., Srinivasan, A., Raghavan, R. V. and Kausalya, M., *J. Geol. Soc. India*, 2000, **55**, 443–445.
8. Jol, H. M. (ed.), *Ground Penetrating Radar Theory and Applications*, Elsevier, Amsterdam, 2009, p. 524.
9. Goel, R. K., *Tunnelling Underground Space Technol.*, 2001, **16**, 63–75.

ACKNOWLEDGEMENTS. We thank members of Engineering Geophysics Division for assistance in the GPR data acquisition. Staff of JHLP is thanked for providing logistical support during the field surveys. Thanks are due to Director, NGRI for encouragement and permission to publish this paper. An anonymous reviewer provided very useful comments that improved the clarity of this paper.

Received 15 March 2010; revised accepted 7 December 2010

D. MYSAIAH*
K. MAHESWARI
M. SRIHARI RAO
P. SENTHIL KUMAR
T. SESHUNARAYANA

*National Geophysical Research Institute
(CSIR),
Uppal Road,
Hyderabad 500 606, India
*For correspondence.
e-mail: dasari_mysaiah@yahoo.co.in*